

## Analysis of p53 Inactivation in a Human T-Cell Leukemia Virus Type 1 Tax Transgenic Mouse Model

TONI PORTIS,<sup>1</sup> WILLIAM J. GROSSMAN,<sup>1</sup> JOHN C. HARDING,<sup>1</sup> JAY L. HESS,<sup>2</sup> AND LEE RATNER<sup>1\*</sup>

*Departments of Medicine, Pathology, and Molecular Microbiology, Washington University School of Medicine, St. Louis, Missouri 63110,<sup>1</sup> and Department of Pathology and Laboratory Medicine, University of Pennsylvania School of Medicine, Philadelphia, Pennsylvania 19104<sup>2</sup>*

Received 18 September 2000/Accepted 6 December 2000

**Human T-cell leukemia virus type 1 (HTLV-1) is the etiologic agent of adult T-cell leukemia/lymphoma (ATLL). The HTLV-1 Tax protein has been strongly linked to oncogenesis and is considered to be the transforming protein of this virus. A Tax transgenic mouse model was utilized to study the contribution of p53 inactivation to Tax-mediated tumorigenesis. These mice develop primary, peripheral tumors consisting of large granular lymphocytic (LGL) cells, which also infiltrate the lymph nodes, bone marrow, spleen, liver, and lungs. Primary Tax-induced tumors and tumor-derived cell lines exhibited functional inactivation of the p53 apoptotic pathway; such tumors and tumor cell lines were resistant to an apoptosis-inducing stimulus. In contrast, p53 mutations in tumors were found to be associated with secondary organ infiltration. Three of four identified mutations inhibited transactivation and apoptosis induction activities in vitro. Furthermore, experiments which involved mating Tax transgenic mice with p53-deficient mice demonstrated minimal acceleration in initial tumor formation, but significantly accelerated disease progression and death in mice heterozygous for p53. These studies suggest that functional inactivation of p53 by HTLV-1 Tax, whether by mutation or another mechanism, is not critical for initial tumor formation, but contributes to late-stage tumor progression.**

Human T-cell leukemia virus type 1 (HTLV-1) is the causative agent of adult T-cell leukemia/lymphoma (ATLL), a highly aggressive and fatal CD4<sup>+</sup> T-lymphoproliferative malignancy that occurs in approximately 1 to 5% of HTLV-1-infected individuals after a long latency period (33). The HTLV-1 Tax protein is a potent transcriptional transactivator of both viral and cellular gene expression. Tax normally exerts its effects on viral gene expression by activating cellular transcription factors which, in turn, bind Tax responsive elements located in the viral long terminal repeat (4). Tax has also been shown to transactivate cellular gene transcription by acting on several structurally unrelated cellular proteins, including cyclic AMP (cAMP) response element/activating transcription factor (CREB/ATF) members, NF- $\kappa$ B/Rel proteins, and serum response factors (1, 10, 11, 13).

It has been suggested that Tax mediates cellular transformation by stimulating proliferation and/or inhibiting apoptosis. Tax upregulates cyclin D2 expression and stimulates G<sub>1</sub>-to-S-phase transition through upregulated CDK4 and CDK6 activity (37, 39). Tax has also been shown to directly bind and affect the activity of a number of cell cycle regulatory proteins, such as p15, p16, and cyclin D3 (27, 29, 41, 42). In transient-transfection experiments, Tax transactivates the proliferating cell nuclear antigen promoter and transrepresses expression of p18 and p56<sup>lck</sup>, as well as the apoptosis-inducing gene *bax*, through E-box elements (3, 23, 35, 42). Other reports indicate that Tax expression induces interleukin 2 (IL-2)-independent proliferation and resistance to apoptosis in IL-2-dependent cutaneous T-cell leukemia/lymphoma type 2 (CTLL-2) cells (17). This

resistance is not associated with repression of *bax* but with transactivation of the antiapoptotic bcl-xl protein through NF- $\kappa$ B elements located in the promoter region (44).

The tumor suppressor protein p53 plays a critical role in cell cycle regulation, DNA repair, and apoptosis. In response to DNA damage, p53 activates a number of genes involved in cell cycle arrest or apoptosis, such as *p21* (WAF1) and *bax* (12, 24). *p53* mutations occur in >50% of all human cancers and in leukemic cells of >30% of ATLL patients. These mutations are associated with the accumulation of additional genetic alterations and chromosomal abnormalities, resulting ultimately in immortalization (6, 30). Certain hot spots of *p53* mutations occur more frequently in particular types of tumors; however, most involve exons 5 through 8, a highly conserved DNA binding domain critical for p53 function (8). Although *p53* is not usually mutated in cells transformed by HTLV-1 in vitro, recent reports have suggested that wild-type p53 protein is stabilized and functionally impaired in these cells, resulting in reduced induction of p53-responsive genes (5, 31, 34). Unlike adenovirus E1B 55K, simian virus 40 large T antigen, and human papillomavirus (HPV) E6 viral proteins, which all bind p53 and inhibit its function, HTLV-1 Tax does not appear to directly interact with p53 (38, 47). Instead, HTLV-1 is thought to alter posttranslational modification of p53, abrogating its function (32).

We have previously demonstrated that expression of HTLV-1 Tax in the mature lymphoid compartment in mice is sufficient for lymphoma development. These mice express Tax from the human granzyme B promoter, limiting its production to cytotoxic T-lymphocyte (CTL) and natural killer (NK) cells. The mice develop primary, peripheral lymphomas at 6 to 9 months of age which infiltrate the lymph nodes, bone marrow, spleen, liver, and lungs (14). Tumor cells demonstrate elevated production of IL-1 $\alpha$ , IL-1 $\beta$ , gamma interferon, granulocyte-

\* Corresponding author. Mailing address: Box 8069, Washington University, 660 South Euclid Ave., St. Louis, MO 63110. Phone: (314) 362-8836. Fax: (314) 747-2797. E-mail: lratner@imgate.wustl.edu.

macrophage colony-stimulating factor (IL-15, IL-10, and IL-6), and constitutive cell surface expression of ICAM-1, LFA-1, and VLA-4 (15; T. Portis and L. Ratner, unpublished data). In this study, we utilized Tax transgenic mice to determine the contribution of p53 inactivation to Tax-induced tumorigenesis. Accumulation of specific mutations in the DNA binding domain of p53 was associated with tumor dissemination. Three of four mutations analyzed were shown to inhibit p53-specific transactivation and apoptosis in vitro. Interestingly, fresh tumors and tumor-derived cell lines from Tax transgenic mice were resistant to irradiation-induced apoptosis; however, transcriptional activation of downstream p53 responsive genes appeared normal. In vivo, we found that tumor formation was not accelerated in p53<sup>+/-</sup> Tax<sup>+</sup> mice compared to that in p53<sup>+/+</sup> Tax<sup>+</sup> mice; however, p53 heterozygosity was associated with formation of multiple tumors and accelerated mortality. This, together with the correlation between frequency of p53 mutation and tumor dissemination, suggests that p53 inactivation is a late event in Tax-mediated tumorigenesis, possibly accounting for rapid dissemination and disease progression. Furthermore, Tax-induced events early in tumorigenesis likely involve inhibition of apoptosis, possibly through downstream effectors in the p53 pathway.

#### MATERIALS AND METHODS

**Mice.** Granzyme B-Tax transgenic mice (Tax<sup>+</sup>) were generated as previously described (14). Mice containing a homozygous deletion in p53 (p53<sup>-/-</sup>) were purchased from Jackson Laboratories (18). Tax<sup>+</sup> mice were mated with p53<sup>-/-</sup> mice, and the resulting p53<sup>+/-</sup> Tax<sup>+</sup> progeny were mated for production of F<sub>2</sub> progeny. F<sub>2</sub> mice were monitored weekly for rates of tumor formation, morbidity, and mortality. Pathological characteristics of tumors were compared among p53<sup>+/+</sup> Tax<sup>+</sup>, p53<sup>+/-</sup> Tax<sup>+</sup>, p53<sup>-/-</sup> Tax<sup>+</sup>, p53<sup>+/+</sup>, p53<sup>+/-</sup>, and p53<sup>-/-</sup> transgenic littermates. All genotyping was performed as described previously (14; Jackson Laboratories protocol). Tissues were fixed in 10% neutral-buffered formalin, embedded in paraffin for sectioning, and stained with hematoxylin and eosin as described previously (14). All mice were bred and maintained under pathogen-free conditions in accordance with Washington University animal care guidelines. Kaplan-Meier analysis and statistical calculations were carried out using the SPSS statistical analysis program (SPSS, Inc.).

**Tissues and cell lines.** Fresh tumors and tissues removed from mice were released into medium supplemented with 10% fetal bovine serum, 1% L-glutamine, 1% sodium pyruvate, and 1% penicillin-streptomycin (RPMI medium; Life Technologies). Erythrocytes in splenocyte preparations were lysed with 155 mM ammonium chloride and washed prior to culture. The tumor-derived F8 and SC large granular lymphocytic (LGL) cell lines have been described elsewhere and were maintained in RPMI medium (14, 15). Abelson murine leukemia virus (MLV)-transformed pre-B-cell lines containing wild-type (204-3-1) and mutant (143-2M) p53 were provided by Naomi Rosenberg (Tufts University, Boston, Mass.) (43) and maintained in RPMI medium. The human H1299 non-small-cell lung carcinoma cell line was provided by Rainer Brachmann (Washington University, St. Louis, Mo.) and maintained in Dulbecco modified Eagle medium (DMEM) (Life Technologies) supplemented with 10% fetal bovine serum, 1% L-glutamine, and 1% sodium pyruvate plus 1% penicillin-streptomycin (called DMEM). The SAOS-2 osteosarcoma cell line was provided by Doug Dean (Washington University) and maintained in DMEM.

**PCR-single strand conformation polymorphism (PCR-SSCP) analysis.** Genomic DNA was extracted from tumor cells in buffer containing 100 mM NaCl, 10 mM EDTA (pH 8), 50 mM Tris-Cl (pH 7.6), 1% sodium dodecyl sulfate (SDS), and 0.5 mg of proteinase K/ml. Following an overnight incubation at 50°C, genomic DNA was phenol-chloroform extracted and precipitated with a 1/10 volume 3 M sodium acetate (pH 5.5) and 2 volumes of ethanol. DNA from nontransgenic mice and cells containing known p53 mutations were used as controls when available (2).

Primers used for amplification of exons 5 to 8 of p53 have been described previously (2). Briefly, 200 ng of genomic DNA was added to reaction mixtures containing 0.15 µg each of sense and antisense primers (IDT, Inc.), 1× PCR buffer, 1 µCi of [ $\alpha$ -<sup>32</sup>P]dCTP (ICN), 0.05 mmol of deoxynucleoside triphos-

phates/liter, 25 mmol of MgCl<sub>2</sub>/liter, and 1 U of *Taq* DNA polymerase (Life Technologies). PCR was run as follows: 3 min at 95°C, 30 cycles of 1 min at 95°C and 1 min at 64°C, and a final extension of 5 min at 64°C. After amplification, PCR products were denatured for 2 min at 94°C and immediately placed on ice. Samples were loaded on 0.75× Mutation Detection Enhancement gels (FMC), run at 8 W in 4°C for 6 h, and exposed to X-ray film.

Mutant DNA fragments were excised from gels, and DNA was eluted in 500 mM ammonium acetate–10 mM magnesium acetate–1 mM EDTA–0.1% SDS. Aliquots of samples were then subjected to another round of PCR-SSCP analysis utilizing the appropriate primers to confirm the absence of wild-type p53 contamination and cloned into PCR-TRAP vectors according to the manufacturer's specifications (GenHunter). Vector-specific primers were utilized for automated, PCR-based sequence analysis (P-Y. Kwok, Washington University). Wild-type p53 sequences from each exon were cloned in parallel for use as controls. The Universal Mutation p53 database (16) was utilized to calculate the number of times each particular mutation has been documented in human cancers.

**RT-PCR and plasmid construct generation.** Total RNA was extracted from wild-type (204-3-1) and mutant (143-2M) p53-containing cell lines using TRI reagent (Sigma). Reverse transcriptase (RT) reactions were performed according to the Superscript II RT protocol (Life Technologies). A portion of the RT product was used in standard PCRs, including 0.5 µg each of p53 sense (S) (5'-GGAATTCAGGCCCTCATCT-3') and antisense (AS) (5'-GGAATTCAGCCCTGAAGTCATAAGA-3') primers containing *Eco*RI linkers to amplify nucleotides 101 to 1399. Site-directed mutagenesis was performed by using PCRs to independently amplify 5' and 3' regions of p53. Primer sets consisted of either sense or antisense primers (above) combined with primers containing single-point mutations. Diluted aliquots (1:100) of the modified 5' and 3' p53 sequences were then combined and reamplified by PCR using p53 sense and antisense primers.

Mutant and wild-type p53 PCR products were cloned into TA vectors and subsequently cloned into pcDNA3 expression vectors at *Eco*RI sites (Invitrogen). All clones were sequenced to verify the presence of specific mutations. Luciferase reporter plasmids were provided by Naomi Rosenberg (Tufts University) (43). The p21p construct contains the complete p21 promoter region upstream of luciferase while p21pΔ1.1 is missing 1.1 kb of the 5' sequence that is specific for p53 transactivation of the p21 promoter (9).

**Transfections, transactivation analysis, and apoptosis studies.** H1299 cells were transfected with 1 µg of p53 expression plasmid and 0.2 µg of reporter plasmid in serum-free medium (Optimem) using Lipofectamine reagent (Life Technologies). pcDNA 3-CAT plasmids (0.2 µg) were cotransfected to measure transfection efficiency by chloramphenicol acetyltransferase (CAT) assay (26). Lipofectamine-DNA precipitates were left in culture medium for 16 h. Cells were then re-fed with DMEM, and 24 h later, cell lysates were analyzed for luciferase activity using a luminometer (MGM Instruments).

SAOS-2 cells were transfected with 5 µg of wild-type or mutant p53 expression plasmids by calcium phosphate precipitation methods described previously (7). Cells were cotransfected with pDsRed1-N1 plasmids containing red fluorescent protein (RFP; Clontech) and p53 expression plasmids and were harvested 36 h posttransfection. RFP-positive apoptotic cells were measured by fluorescence labeling of fragmented DNA using the FlowTACS FITC protocol (Trevigen, Inc.). Dual positive cells were analyzed by fluorescence-activated cell sorter (FACS) analysis on a FACScan flow cytometer (Becton Dickinson).

Fresh tumor suspensions were treated with 2,000 rads of  $\gamma$ -irradiation and placed in RPMI medium. Five hours postirradiation, 10<sup>5</sup> cells were stained with fluorescein isothiocyanate (FITC)-conjugated antibody against annexin V as described by the manufacturer (Pharmingen). Apoptotic cells were measured by FACS analysis on a FACScan flow cytometer (Becton Dickinson). Total RNA was also extracted 2 h postirradiation using TRI reagent, and RT-PCRs were performed as described above using primers specific for p21, bax, mdm2, p53, GAPDH (glyceraldehyde-3-phosphate dehydrogenase), and HGPRT (hypoxanthine/guanine phosphoribosyl transferase). The primers and sequences were as follows: p21 S (5'GGTCCCGTGGACAGTGAGCA-3') and p21 AS (5'-GTCA GGCTGGTCTGCTCCG-3'), bax S (5'-CCAGTCTGAACAGATCATG-3') and bax AS (5'-TCAGCCCATCTTCTCCAGA-3'), mdm2 S (5'-CAAGCAC CTCACAGATTCCA-3') and mdm2 AS (5'CATCCTCATCTGAGAGCTCG-3'), and GAPDH S (5'-CCATCACCATCTTCCAGGAGCGAG-3') and GAPDH AS (5'-CACAGTCTTCTGGGTGGCAGTGAT-3'). PCR products were separated by electrophoresis and visualized by UV light exposure. Fold activation of transcripts was quantitated by normalizing the intensities of p21, bax, mdm2, and p53 products to that of GAPDH.

**Western blottings.** Total cellular protein was prepared by lysing cells in a mixture containing 50 mM Tris-Cl (pH 7.5), 5 mM EDTA, 150 mM NaCl, 1% Triton X-100, 10 µg of aprotinin/ml, 0.5 mM phenylmethylsulfonyl fluoride, and

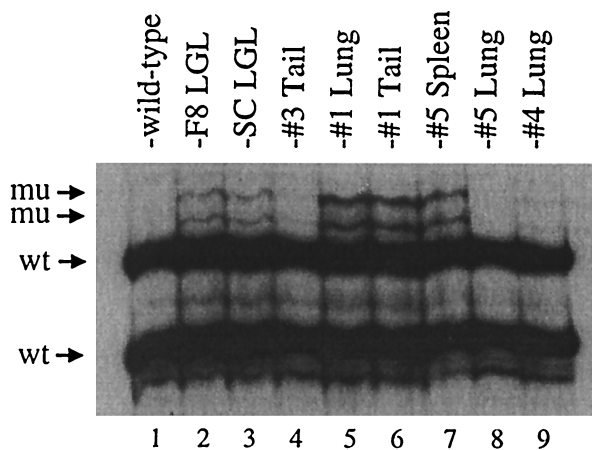


FIG. 1. Identification of mutated p53 alleles in tumors from Tax transgenic mice. PCR-SSCP analysis was performed on tumors and IL-2-independent tumor-derived cell lines from Tax transgenic mice using primers specific for exons 1, 5, 6, 7, and 8 of murine p53. This representative PCR-SSCP gel of exon 6 shows the migration of wild-type p53 (wt) from nontransgenic tail DNA (lane 1) and mutated p53 (mu) in tumors (lanes 4 to 9) and tumor-derived cell lines (lanes 2 and 3) from Tax transgenic mice.

5 µg of pepstatin/ml. Five micrograms of protein was immunoprecipitated with monoclonal antibodies specific for mutant p53 (Ab-3) and wild-type p53 (Ab-11) (both from Oncogene Sciences) or pooled anti-Tax monoclonal antibodies (no. 168A51-2, 168A51-42, and 168B17-46-34; AIDS Reagent Program, Rockville, Md.). Immunoprecipitated proteins were fractionated on SDS-10% acrylamide denaturing gels and electroblotted to nitrocellulose membranes by standard techniques (MSI). Immunoblotting was performed using antibodies to p53 or Tax diluted 1:500, followed by treatment with goat anti-mouse alkaline phosphatase-conjugated secondary antibody (1:3,000; Sigma) and visualization by enhanced chemiluminescence (Amersham).

RESULTS

**p53 mutations are present in tumors from Tax transgenic mice.** Since p53 mutations have been documented in tumors from ATLL patients, we utilized PCR-SSCP analysis to determine whether similar mutations are present in tumors from HTLV-1 Tax transgenic mice. Genomic DNA from a panel of tumors and tumor-derived cell lines was used for this PCR-based assay, which detects conformational intrastrand differences in DNA with a different sequence. The primers used were specific for exon 1 and exons 5 to 8 of murine p53. Exons 5 to 8 comprise the p53 core domain, which contains sequence-specific DNA binding activity and is necessary for transactivation of genes involved in cell cycle arrest and apoptosis. Studies have shown that most p53 point mutations occur in this region and result in the loss of functional p53 due to destabilization of the three-dimensional protein structure (8).

A representative PCR-SSCP gel of exon 6, showing migration of wild-type and mutant p53 DNA strands in tumors from Tax transgenic mice, is presented in Fig. 1. The majority of p53 genes appear to be wild type, which may reflect the heterogeneity of the tumor samples or the fact that the mutations are not present in the majority of tumor cells or are only in one allele of p53. Spleen and lung tissue also contain significant numbers of normal, nonmalignant cells; however, biological clones grown from tumors show the same predominance of wild-type p53 (data not shown). Mutations concentrated in

exons 5 to 8 of p53 were initially identified by PCR-SSCP analysis in 3 of 7 primary, peripheral tumors (43%) and 10 of 11 sites of dissemination (91%), including spleen, lymph nodes, lung, and liver (Table 1). No mutations were found in the less mutable exon 1 of p53 in any of the mice tested (data not shown). Two tumor-derived LGL cell lines, F8 and SC, developed IL-2 independence after prolonged growth in vitro (15). The cell lines exhibited the same mutations in exons 6 and 7 of p53 (Fig. 1 and data not shown). These data suggest a correlation between p53 mutation and late-stage tumor progression.

Abnormally migrating bands on PCR-SSCP gels were then extracted, subjected to another round of PCR-SSCP analysis, cloned into plasmid vectors, and sequenced. Although sequence analysis determined that various point mutations were present throughout the p53 core domain, four specific mutations in exons 6 and 7 arose frequently in tumors from several Tax transgenic mice (Table 1). These mutations included P203A, E228G, N239S, and G244R. DNA from tumor samples was digested with enzymes specific for restriction sites either generated or deleted as a result of mutation in order to verify that they were indeed present in genomic DNA (data not shown). Some primary and disseminated tumors contained more than one p53 mutation; however, only one exon at a time could be analyzed, making it difficult to determine the relative levels of each mutation in tumor samples. The IL-2-independent F8 and SC tumor-derived cell lines contained both P203A and N239S mutations.

The Universal Mutation p53 database, which documents more than 10,000 p53 mutations occurring in human cancers (16), was utilized to calculate the number of times a nucleotide change has been documented at that location. As shown in Table 1, these residues are frequent sites of mutation in human cancers. The P203A and E228G mutations are located at critical turns between highly twisted β-strands of the p53 core domain while the N239S and G244R mutations are located in the L3 loop, a critical area of p53 protein-DNA contact and frequent site of mutation (8).

TABLE 1. p53 mutations in Tax-induced tumors

Mutation <sup>a</sup>	Frequency	No. documented <sup>b</sup>
Primary tumors	3/7 (43%) <sup>c</sup>	
P203A	2/7 (29%)	
N239S	2/7 (29%)	
Disseminated tumors	10/11 (91%) <sup>d</sup>	
P203A	3/11 (27%)	25
E228G	5/11 (45%)	19
N239S	3/11 (27%)	68
G244R	3/11 (27%)	106

<sup>a</sup> Primary and disseminated tumor tissues from a total of seven different mice were analyzed for p53 mutations. Except for positions 203 (Ala in murine p53 and Val in human p53) and 228 (Gly in murine p53 and Asp in human p53), the amino acid sequences are identical in murine and human p53.

<sup>b</sup> The Universal Mutation p53 database, which contains over 10,000 p53 mutations identified in all types of human cancers, was utilized to calculate the number of times a nucleotide change has been identified at that location.

<sup>c</sup> One primary tail tumor contained both P203A and N239S mutations, and two tumors contained either a P203A or N239S mutation.

<sup>d</sup> Two disseminated tumors contained both E228G and N239S mutations and two contained both P203A and E228G.

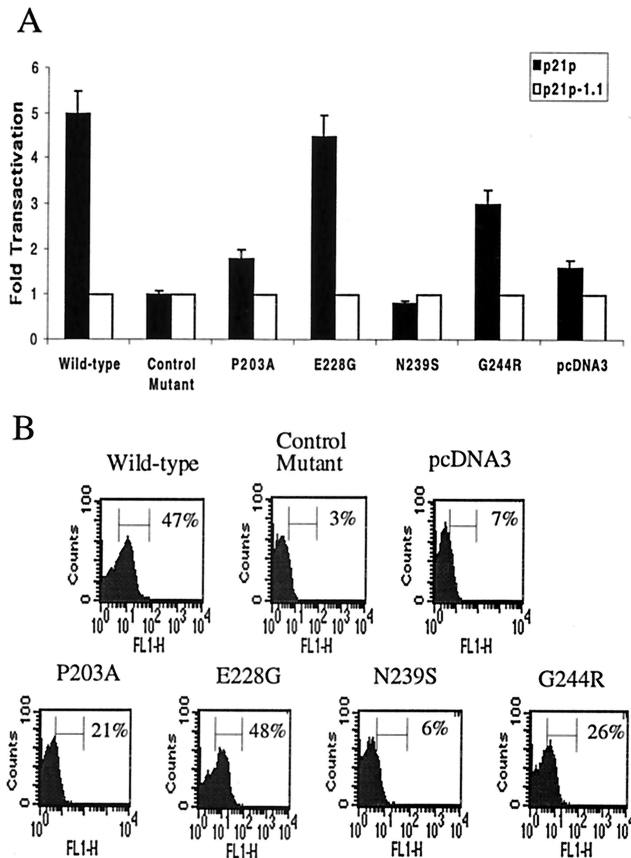


FIG. 2. Individual p53 mutants demonstrate variable levels of p53 specific transactivation and apoptosis. (A) Mutant and wild-type p53 expression vectors were cotransfected into H1299 cells with luciferase constructs containing (p21p) or lacking (p21pΔ1.1) p53-responsive elements. PCR amplification of a known mutant p53 species (143-2M) containing a C170W mutation in exon 5 was performed in parallel. Background transactivation of constructs lacking p53 response elements was set to a value of 1. (B) Mutant and wild-type p53 expression vectors and RFP-expressing plasmids were cotransfected into SAOS-2 cells by calcium phosphate precipitation (7). At 36 h posttransfection, apoptosis was measured by labeling the ends of fragmented DNA with FITC. RFP-positive cells were gated the percentage of cells dual positive for RFP and FITC are shown.

**Individual mutations inhibit p53 function in vitro.** In order to examine the effects of the individual mutations on p53 transactivation and induction of apoptosis, we recreated each mutation separately by PCR-based site-directed mutagenesis. The resulting mutant p53, as well as wild-type p53, DNA sequences were cloned into pcDNA3 expression plasmids. A functionally inactive p53 mutant (C170W) from the 143-2M cell line was cloned in parallel (43). The p53 expression plasmids were cotransfected into p53 null H1299 cells along with constructs expressing the luciferase gene under the p53 responsive p21 promoter (p21p) (9). Identical luciferase constructs lacking the p53-specific response element (p21pΔ1.1) (9) were used as controls for specificity of p53 transactivation. Equivalent levels of p53 expression and transfection efficiency were verified by Western blot analysis and CAT assay, respectively (data not shown). As shown in Fig. 2A, wild-type p53-specific transactivation of p21p was fivefold over that of the deletion construct,

p21pΔ1.1, whereas the control mutant (C170W) transactivated both promoters equally well. The N239S mutant displayed transactivation levels similar to that of the control mutant. The E203A and G244R mutants displayed lower (1.8- to 3-fold) levels than wild-type p53, while the E228G mutation did not appear to be defective in transactivation activity.

We performed additional experiments to determine whether these specific mutations affected the ability of p53 to induce apoptosis in another p53 null cell line, SAOS-2. Cells were cotransfected with p53 expression constructs and RFP-expressing plasmids, and the amount of fragmented DNA indicative of apoptosis in RFP-positive cells was measured by FACS. As shown in Fig. 2B, the P203A, N239S, and G244R mutants were inhibited in their ability to induce apoptosis, similar to the known p53 mutant. In contrast, the E228G mutant induced apoptosis to levels similar to wild-type p53. Therefore, three of these p53 mutations inhibit the ability of p53 to transactivate the p21 promoter and induce apoptosis in an in vitro transfection system.

**Wild-type and mutant p53 protein is expressed in tumors from Tax transgenic mice.** We analyzed protein levels of p53 in tumors and tumor-derived LGL cell lines from Tax transgenic mice by Western blot analysis (Fig. 3). Cell lysates were immunoprecipitated and immunoblotted with conformation-dependent monoclonal antibodies which recognize either wild-type p53 (upper panel) or mutant p53 (middle panel) or monoclonal antibodies against HTLV-1 Tax (lower panel). Most point mutations in p53 dramatically disrupt its secondary structure, allowing for recognition by conformation-dependent antibodies (8). As shown in Fig. 3, both wild-type and mutant p53 are expressed in tumors from Tax transgenic mice. Tax expression appears to be restricted to primary tail and ear

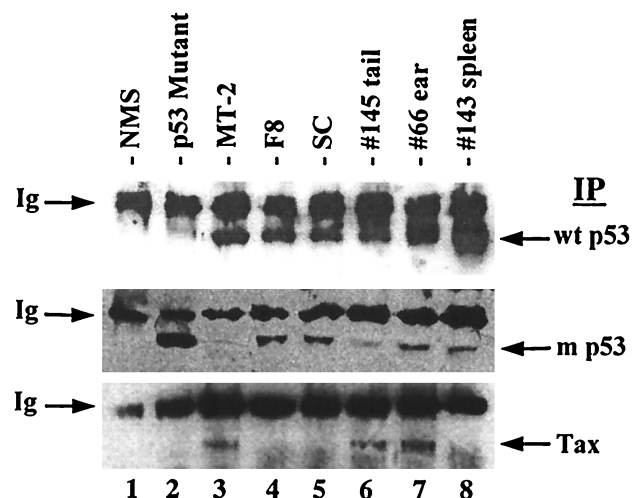


FIG. 3. Expression of wild-type and mutant p53 in tumors from Tax transgenic mice. Cell lysates from tumor-derived cell lines (lanes 4 and 5) and fresh tumors from Tax transgenic mice (lanes 6 to 8) were immunoprecipitated (IP) and immunoblotted with conformation-dependent antibodies specific for wild-type p53 (top), mutant p53 (middle), or HTLV-1 Tax (bottom). Wild-type p53-containing, HTLV-1-transformed T cells (MT2), mutant p53-containing, HTLV-1-transformed T cells (143-2M), and normal mouse splenic tissue (NMS) were utilized as controls. The upper band in each panel represents mouse heavy-chain immunoglobulin (Ig) in each sample.

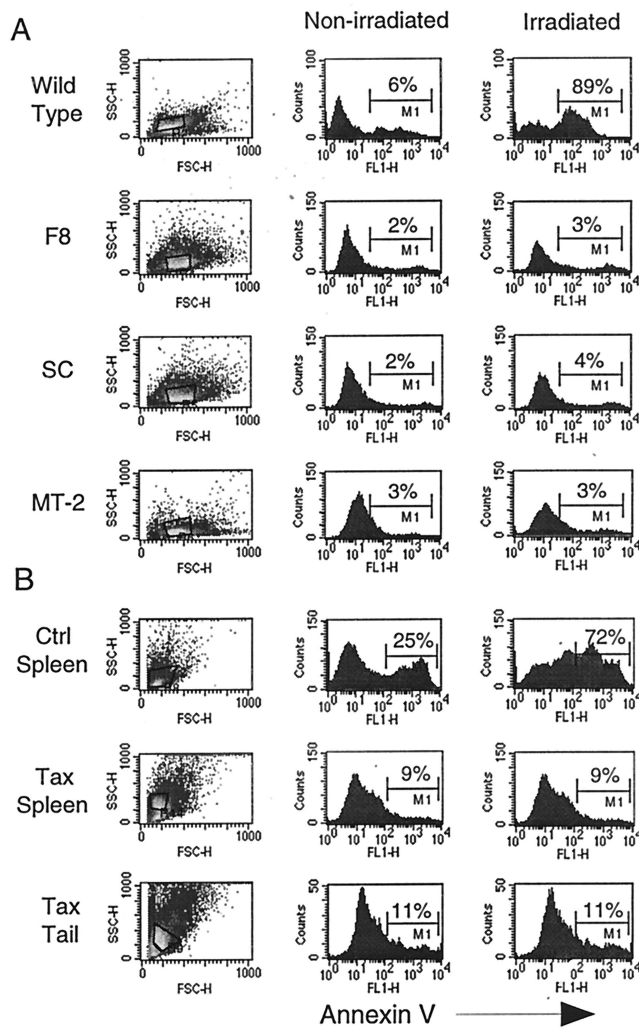


FIG. 4. Tumors from Tax transgenic mice are resistant to irradiation-induced apoptosis. Tumor-derived cell lines (F8 and SC) (A) and fresh tumor cells from Tax transgenic mice (B) were either mock treated (middle column) or exposed to 2,000 rads of  $\gamma$ -irradiation (right column). Five hours later, cells were stained with FITC-conjugated antibodies to annexin V to measure apoptosis. A wild-type p53-containing cell line (204-3-1) and normal mouse splenocytes (Ctrl Spleen) were used as positive controls. The apoptosis-resistant cells consist of the larger, more numerous cells present in spleen and tumor tissue from Tax transgenic mice and absent in normal mouse spleens (compare scatter plots; left).

tumors and absent in spleens (lanes 6 to 8). We have previously shown that the F8 and SC tumor-derived cell lines expressed Tax upon initial isolation; however, Tax expression was undetectable once cells acquired IL-2 independence (15; Fig. 3, lanes 4 and 5). These data suggest an inverse correlation between frequency of p53 mutation or tumor progression and Tax expression.

**Tax-induced tumors are resistant to apoptosis.** To determine the functional status of p53 in fresh tumors and tumor-derived cell lines, we measured their sensitivity to irradiation-induced apoptosis (Fig. 4). The levels of annexin V, an early marker of apoptosis, were measured 5 h after mock or  $\gamma$ -irradiation treatment. Nonirradiated and irradiated controls ex-

hibited between 6 and 25% and 89 and 72% annexin V-positive cells, respectively. As shown in Fig. 4A, the F8 and SC tumor-derived cell lines are completely resistant to apoptosis, similar to HTLV-1-transformed MT2 cells, which are known to contain inactive p53 (34). Similarly, spleen and tail tumor cells from Tax transgenic mice are also resistant to irradiation-induced apoptosis (Fig. 4B), suggesting that p53 is functionally inhibited, whether by mutation or an alternative mechanism. It was determined by scatter plot analysis of tumor cells that the apoptosis-resistant cells consist primarily of the larger, more numerous cells that are present in spleen and tumor tissue from Tax transgenic mice and absent in normal mouse spleens (Fig. 4B, left column). These cells are Fc $\gamma$ IIIR positive, a marker for the LGL cells that make up tumors in Tax transgenic mice (reference 15 and data not shown).

**p53 is transcriptionally active in Tax-induced tumors.** To test the ability of p53 to transactivate downstream genes, total cellular RNA was also isolated from nonirradiated and irradiated tumor cells at 2 h postirradiation. RT-PCRs were carried out to detect levels of p21, bax, mdm2, and p53 mRNA (Fig. 5). Levels of GAPDH were normalized in order to quantitate the fold activations of p21, bax, mdm2, and p53 transcripts following irradiation (Table 2). As expected, upregulation of all transcripts ranged from 3- to 10-fold in cells containing wild-type p53 (Fig. 5, lanes 1 and 2 and 11 and 12; Table 2) and was not observed in cells which express either no p53 or mutant p53 (Fig. 5, lanes 3 to 6; Table 2) following  $\gamma$ -irradiation. Upregulation of all transcripts was also observed in the tumor-derived F8 and SC cell lines (Fig. 5, lanes 7 to 10; Table 2) as well as

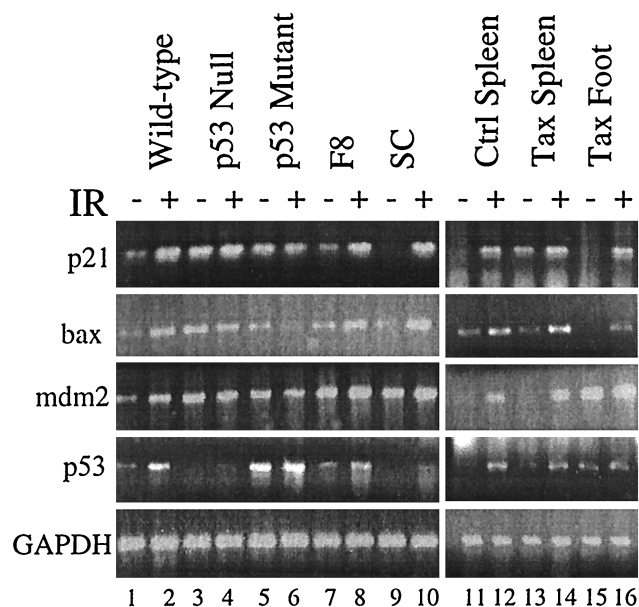


FIG. 5. p53 transactivation activity is functional in Tax-induced tumors and tumor-derived cell lines. Total cellular RNA was isolated from nonirradiated (-) and irradiated (IR) (+) cells at 2 h postirradiation. RT-PCRs were performed using primers specific for p21, bax, mdm2, and p53 mRNA. Levels of GAPDH were measured in parallel to demonstrate that equivalent amounts of RT product were used in each reaction. Cells containing wild-type p53 (204-3-1), mutant p53 (143-2M), and no p53 (L1-2) were utilized as controls to measure p53 transactivation activity.

TABLE 2. p53 transactivation in Tax-induced tumors

Cell type	Fold activation Following IR <sup>a</sup>			
	p21	bax	mdm2	p53
p53 wild type	4.5	3.5	3	5
p53 null	1.1	0.9	1	1.1
p53 mutant	0.9	0.5	1	1.1
F8	4	3	1.5	3
SC	20	4.5	1.5	2.9
Control spleen	10	3	3	4
Tax spleen	4	3	4	3
Tax foot	10	7.5	2	2

<sup>a</sup> Total RNA isolated from nonirradiated and irradiated cells was utilized in RT-PCRs with primers specific for p21, bax, mdm2, and p53 mRNA (Fig. 5). Levels of GAPDH were measured in parallel and normalized to calculate the fold activation of each transcript following  $\gamma$ -irradiation (IR). The fold activation averages of three separate experiments are shown.

tumors (Fig. 5, lanes 13 to 16; Table 2) from Tax transgenic mice. It is difficult to accurately assess transcriptional activation in Tax spleen cells due to the presence of normal, non-malignant cells; however, p53-mediated transactivation did not appear to be lower than that in control spleen cells (three- to fourfold) except in the case of p21 (Table 2). These results were surprising, given the fact that tumors were resistant to apoptosis, and suggest that the presence of p53 mutations in tumors does not affect the normal transactivation function of p53 following  $\gamma$ -irradiation.

**Tumorigenesis in p53<sup>+/-</sup> Tax<sup>+</sup> mice progeny.** To determine if the loss of functional p53 contributes to tumor formation in vivo, we bred Tax transgenic mice with homozygous p53 mutant mice (18). F<sub>1</sub> progeny (p53<sup>+/-</sup> Tax<sup>+</sup>) were then mated for production of F<sub>2</sub> progeny. Mice with homozygous p53 mutations develop a variety of malignancies and die as early as 6 months of age. Tumors arising in p53<sup>-/-</sup> mice include sarcomas and CD4<sup>+</sup> CD8<sup>+</sup> lymphomas, which can be distinguished from Tax transgenic LGL tumors (18).

By histological analysis, we found that p53<sup>-/-</sup> Tax<sup>+</sup> mice develop tumors at the same rate as, and which are identical in histology to those of, p53<sup>+/-</sup> mice, particularly large-cell non-Hodgkin's lymphomas in the spleen and liver, distinct from Tax-induced tumors (data not shown). None of the p53<sup>-/-</sup> Tax<sup>+</sup> mice developed Tax-induced LGL tumors, and the mice died before the normal onset of Tax tumors; thus, we were unable to use these mice in our analysis (Fig. 6A). However, we would have expected to see development of Tax tumors in some of the mice before death if p53 inactivation was a critical obstacle to overcome for tumor development. Instead, we compared the rate of initial tumor formation in p53<sup>+/-</sup> Tax<sup>+</sup> mice to that of p53<sup>+/+</sup> Tax<sup>+</sup> mice. Tax-induced peripheral tumors formed in 100% of these mice. In agreement with in vitro p53 transactivation experiments, we observed only a slight acceleration in tumor formation, which was not statistically significant ( $P < 0.2$ ), in p53<sup>+/-</sup> Tax<sup>+</sup> mice compared to that in mice transgenic for Tax alone. This would suggest that Tax-induced inactivation of p53 is not required for initial tumor development (Fig. 6A).

When we then monitored tumor progression beginning from the time of initial tumor formation, we observed that mice heterozygous for p53 developed peripheral LGL tumors at

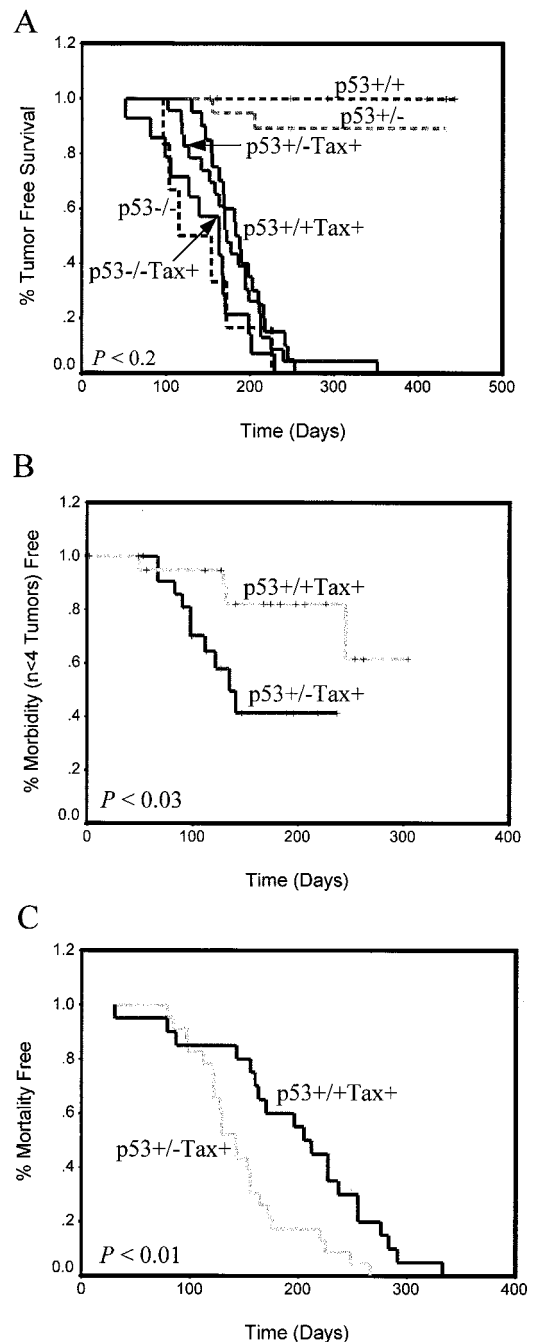


FIG. 6. Tumor initiation and progression in progeny from p53<sup>+/-</sup> Tax<sup>+</sup> transgenic mice. Tax transgenic mice (solid lines) were mated with p53<sup>-/-</sup> mice, and F<sub>1</sub> progeny (p53<sup>+/-</sup> Tax<sup>+</sup>) were mated for production of F<sub>2</sub> progeny. (A) The percent tumor-free survival is plotted as a function of age. Animals were monitored weekly for tumor formation, morbidity, or spontaneous death over a period of 9 months. Except for p53<sup>-/-</sup> Tax<sup>+</sup> ( $n = 14$ ) and p53<sup>-/-</sup> ( $n = 5$ ) mice, at least 20 mice were used for each comparison. The percent morbidity-free (development of fewer than four visible tumors;  $n < 3$ ) survival (B) and the percentage of mortality-free mice (C) were measured from the time of initial tumor formation.

four or more sites ( $P < 0.03$ ) (Fig. 6B) and died significantly earlier ( $P < 0.01$ ) (Fig. 6C) than mice containing wild-type *p53* alleles. These results, taken together, indicate that abrogation of *p53* activity by Tax is not required for initial tumor formation. Rather, Tax may specifically inhibit other components of the *p53* pathway to induce cellular resistance to apoptosis. Furthermore, loss of *p53* function, whether by mutation or another method, likely contributes to rapid dissemination and increased mortality of mice once tumors are established.

## DISCUSSION

There are considerable data suggesting that the HTLV-1 Tax protein induces tumorigenesis by deregulation and functional inhibition of cellular proteins, including components of the *p53*/Rb pathway. We have utilized a Tax transgenic mouse model to determine the contribution of *p53* inactivation to Tax-induced tumorigenesis. Our results suggest that Tax expression in an *in vivo* mouse model of tumorigenesis does not affect the transactivation function of *p53* and that *p53* inactivation, whether by mutation or other method, does not contribute to accelerated tumor formation. These findings differ from those of Pise-Masison et al., which demonstrate inhibition of *p53*-mediated transcriptional activation and apoptosis in HTLV-1-immortalized cell lines (31, 32). The differences may reflect the two distinct model systems used: one utilizes a mouse model of Tax expression and the other utilizes HTLV-1-immortalized human cells. We have not looked at altered phosphorylation of *p53* as a mechanism of Tax inhibition in our system, given the fact that *p53* appears to function normally when activated by  $\gamma$ -irradiation. Thus, we cannot rule out this possibility, especially since  $\gamma$ -irradiation induces a series of downstream phosphorylation events which may override any inhibition induced by Tax (12).

By PCR-SSCP analysis, we identified specific mutations in the critical DNA binding domain of *p53* in tumors from Tax transgenic mice. We initially identified *p53* mutations in 43% of primary, peripheral tumors and 91% of sites of organ infiltration. Four specific mutations in exons 6 and 7 of *p53* were further characterized since their high frequency of occurrence indicated that they were not PCR artifacts. These mutations were confirmed by restriction enzyme digestion of genomic DNA; moreover, mutant *p53* protein expression in tumors and tumor-derived cell lines was identified by Western blot analysis. Three of these mutations, although inhibitory in an *in vitro* transfection system, apparently are not predominant enough in tumors to abrogate *p53* transactivation of downstream *p53* responsive genes following  $\gamma$ -irradiation. However, it is possible that these mutations may be inhibitory under more physiologic conditions of stress.

Our results are similar to those utilizing Abelson MLV-transformed pre-B cells, in which inhibitory mutations clustered within the *p53* core domain were generated late in transformation and appeared not to be required for initial transformation. However, unlike the Tax-induced tumors in our system, MLV-transformed cells predominantly expressed mutant *p53*, which is unable to activate *p21* transcription or induce apoptosis following irradiation (43). In our system, tissues containing disseminated tumor cells also harbored large numbers of nonmalignant cells, which made it difficult to mea-

sure the percentage of tumor cells containing specific *p53* mutations. The presence of *p53* mutations in the IL-2-independent tumor-derived cell lines from Tax transgenic mice supports the idea that late-stage genetic mutations in *p53* may allow cells to grow without exogenous cytokines. However, if these mutations provide a growth advantage for tumor cells, it is expected that organ-infiltrating tumor cells would be clonal and contain predominantly mutant *p53*. This was not observed when biological clones were cultured from tumors, suggesting that these mutations do not need to be selected for tumor outgrowth *in vitro*. An alternative explanation is supported by the finding that Tax inhibits nucleotide excision repair, presumably through increased proliferating cell nuclear antigen expression (21, 35). This may predispose cells to accumulation of DNA damage and spontaneous mutation, an event that has been attributed to Tax expression (28).

Despite the fact that *p53* transactivation activity is normal, the apoptotic pathway appears to be inactive in tumors and tumor-derived cell lines from Tax transgenic mice, based upon their resistance to  $\gamma$ -irradiation. Additionally, only the larger tumor cells present in spleen and tail tumors were resistant to apoptosis. The smaller lymphoid cells were sensitive to apoptosis, similar to cells present in normal control mouse spleens. In support of our findings, resistance to Fas-mediated apoptosis in spleen cells has also been associated with escape of autoreactive T cells and development of autoimmune disease in HTLV-1 transgenic mice (22).

In addition to transcription-dependent *p53*-mediated apoptosis, a transcription independent pathway of apoptosis has been described. This pathway is thought to involve the proline-rich region of *p53*, located between the central DNA binding domain and the 5' transactivation domain. This region mediates binding of *p53* to proteins containing SH3 domains and is thought to be involved in induction of apoptosis, yet dispensable for *p53*-mediated transactivation (24, 36). This pathway, largely Tax independent, is suggested to involve additional signals or cofactors necessary for apoptosis or suppression of a survival factor needed to inhibit the actions of Tax (36). We have not ruled out the possibility that mutations in this region of *p53* may be present in Tax-induced tumors or that Tax disrupts protein-protein interactions involving this region, independent of mutation.

Another possibility is that Tax inhibits downstream effectors of *p53* necessary for apoptosis. For instance, resistance to apoptosis induced by the Epstein-Barr virus LMP-1 protein is associated with expression of the anti-apoptotic *bcl-2* and *A20* proteins, which are regulated by NF- $\kappa$ B activation. In fact, it has been suggested that a critical balance between pro- and antiapoptotic *bcl-2* family members regulates apoptosis (40). Along these lines, studies have shown that Tax can transrepress expression of the apoptosis-promoting protein *bax* and can transactivate expression of the antiapoptotic protein *bcl-xl*, most likely through the NF- $\kappa$ B elements in the *bcl-xl* promoter. This action is associated with development of IL-2 independence in CTLL-2 cells (3, 17, 44). To our knowledge, Tax-mediated inhibition of other essential downstream components of *p53*-mediated apoptosis has not been researched. Herpes simplex virus-1, for example, has been shown to specifically inhibit both caspase-8 and caspase-3 activity following induction of apoptosis (19).

The finding that tumor formation in  $p53^{+/-}$  Tax<sup>+</sup> mice was not significantly accelerated compared to that of  $p53^{+/+}$  Tax<sup>+</sup> mice supports our *in vitro* p53 transactivation data. p53 functions primarily as a tetramer, and it has been shown that a mere reduction in p53 levels may promote tumorigenesis; therefore, an increased rate of Tax-induced tumor formation in p53 heterozygous mice would have been observed if p53 inactivation contributed to tumor formation (46). In fact, a recent study by Li et al. demonstrates that  $p53^{+/-}$  mice transgenic for HPV E6 and E7 develop a novel lymphomagenesis, which is not observed in  $p53^{+/+}$  E6 and E7 or  $p53^{+/-}$  mice, at 3 to 6 months of age. This suggests that p53 inactivation from degradation by HPV E6 and E7 is important for tumor development in these animals (25). Tumors developing in  $p53^{-/-}$  Tax<sup>+</sup> mice are identical to those of  $p53^{-/-}$  mice and arise earlier than tumors induced by Tax alone (3 to 5 months versus 6 to 9 months). Again, we would expect to see development of Tax-induced peripheral tumors sometime before death of the mice if p53 inactivation was an obstacle to overcome for tumor formation. This is in contrast to studies involving infection of p53-deficient mice with Abelson MLV. These mice demonstrated a shortened latency period before tumor formation, suggesting that p53 inactivation is important for tumor development induced by this virus (45). Similarly, using a Wnt-1 mouse mammary tumor model, Jones et al. have shown that p53 deficiency contributes to accelerated tumor development (20).

When we then monitored tumor progression in  $p53^{+/-}$  Tax<sup>+</sup> and  $p53^{+/+}$  Tax<sup>+</sup> mice, beginning from the time of initial tumor formation, we observed formation of multiple tumors ( $n > 3$ ) and accelerated mortality in Tax transgenic mice heterozygous for p53. The tumors were identical to those induced by Tax alone and distinct from late-stage tumors described for  $p53^{+/-}$  mice (18). This suggests that, once tumors are established, p53 inactivation allows for a more aggressive disease course, resulting in rapid dissemination and death. Our results are supported by the observation that, since p53 can be induced by hypoxia, the presence of a rich blood supply early in tumor development (i.e., leukemia/lymphoma) results in late selection for p53 inactivation in tumors (24). Additionally, a study of erythroleukemias induced by Friend MLV suggests that p53 inactivation does not directly immortalize cells but promotes accumulation of mutations that lead to accelerated tumor progression *in vivo* (48). Taken together, these results suggest that p53 inactivation by Tax, whether by mutation or another mechanism of inhibition, is not critical for initial tumor formation. Rather, p53 inactivation likely occurs late in tumorigenesis and may be responsible for rapid dissemination and the extremely aggressive and fatal course of ATLL.

We propose that Tax expression in our mouse model induces uncontrolled entry into the cell cycle (29, 37, 39, 42) and inhibits apoptosis induced by DNA damage (32, 44) while disrupting DNA repair systems (21, 35). Our RT-PCR results suggest that this occurs either independent of or downstream of p53. After cells enter a transformed state, p53 is likely inactivated, either by genetic damage or a more direct mechanism, leading to rapid tumor dissemination and death as demonstrated in  $p53^{+/-}$  Tax<sup>+</sup> mice. Future studies will utilize this transgenic-mouse model to identify the initial events in

HTLV-1 Tax-mediated tumorigenesis, specifically with regard to inhibition of the apoptotic pathway.

#### ACKNOWLEDGMENTS

We thank Naomi Rosenberg, Doug Dean, and Rainer Brachmann for reagents and technical support.

This work was supported by National Institutes of Health grants CA-63417 and RR-14324, a National Heart Lung and Blood Institute National Research Service Award, and a Leukemia and Lymphoma Society fellowship.

#### REFERENCES

1. Arima, N., J. A. Molitor, M. R. Smith, J. H. Kim, Y. Daitoku, and W. C. Greene. 1991. Human T-cell leukemia virus type I Tax induces expression of the Rel-related family of kappa B enhancer-binding proteins: evidence for a pretranslational component of regulation. *J. Virol.* **65**:6892-6899.
2. Brathwaite, O., W. Bayona, and E. W. Newcomb. 1992. p53 mutations in C57BL/6J murine thymic lymphomas induced by gamma-irradiation and N-methylnitrosourea. *Cancer Res.* **52**:3791-3795.
3. Brauweiler, A., J. E. Garrus, J. C. Reed, and J. K. Nyborg. 1997. Repression of Bax gene expression by the HTLV-1 Tax protein: implications for suppression of apoptosis in virally infected cells. *Virology* **231**:135-140.
4. Cann, A. J., J. D. Rosenblatt, W. Wachsmann, N. P. Shah, and I. S. Y. Chen. 1985. Identification of the gene responsible for human T-cell leukemia virus transcriptional regulation. *Nature* **318**:571-574.
5. Cereseto, A., F. Diella, J. C. Mulloy, A. Cara, P. Michieli, R. Grassmann, G. Franchini, and M. E. Klotman. 1996. p53 functional impairment and high p21 (waf1/cip1) expression in human T-cell lymphotropic/leukemia virus type I-transformed T cells. *Blood* **88**:1551-1560.
6. Cesarman, E., A. Chadburn, G. Inghirami, G. Gaidano, and D. M. Knowles. 1992. Structural and functional analysis of oncogenes and tumor suppressor genes in adult T-cell leukemia/lymphoma shows frequent p53 mutations. *Blood* **80**:3205-3216.
7. Chen, C., and H. Okayama. 1987. High-efficiency transformation of mammalian cells by plasmid DNA. *Mol. Cell. Biol.* **7**:2745-2752.
8. Cho, Y., S. Gorina, P. D. Jeffrey, and N. P. Pavletich. 1994. Crystal structure of a p53 tumor suppressor-DNA complex: understanding tumorigenic mutations. *Science* **265**:346-355.
9. Datto, M. B., Y. Li, J. F. Panus, D. J. Howe, Y. Xiong, and X.-F. Wang. 1995. Transforming growth factor beta induces the cyclin-dependent kinase inhibitor p21 through a p53-independent mechanism. *Proc. Natl. Acad. Sci. USA* **92**:5545-5549.
10. Franchini, G. 1995. Molecular mechanisms of human T-cell leukemia/lymphotropic virus type I infection. *Blood* **86**:3619-3639.
11. Fujii, M., T. Niki, T. Mori, T. Matsuda, M. Matsui, N. Nomura, and M. Seiki. 1991. HTLV-1 Tax induces expression of various immediate early serum responsive genes. *Oncogene* **6**:1023-1029.
12. Giaccia, A. J., and M. B. Kastan. 1998. The complexity of p53 modulation: emerging patterns from divergent signals. *Genes Dev.* **12**:2973-2983.
13. Giebler, H. A., J. E. Loring, K. van Orden, M. A. Colgin, J. E. Garrus, K. W. Escudero, A. Brauweiler, and J. K. Nyborg. 1997. Anchoring of CREB binding protein to the human T-cell leukemia virus type I promoter: a molecular mechanism of Tax transactivation. *Mol. Cell. Biol.* **17**:5156-5164.
14. Grossman, W. J., J. T. Kimata, F. H. Wong, M. Zutter, T. J. Ley, and L. Ratner. 1995. Development of leukemia in mice transgenic for the tax gene of human T-cell leukemia virus type I. *Proc. Natl. Acad. Sci. USA* **92**:1057-1061.
15. Grossman, W. J., and L. Ratner. 1997. Cytokine expression and tumorigenicity of large granular lymphocytic leukemia cells from mice transgenic for the tax gene of human T-cell leukemia virus type I. *Blood* **90**:783-794.
16. Hollstein, M., K. Rice, M. S. Greenblatt, T. Soussi, R. Fuchs, T. Sorlie, E. Hovig, B. Smith-Sorensen, R. Montesano, and C. C. Harris. 1994. Database of p53 gene somatic mutations in human tumors and cell lines. *Nucleic Acids Res.* **22**:3551-3555.
17. Iwanaga, Y., T. Tsukahara, T. Ohashi, Y. Tanaka, M. Arai, M. Nakamura, K. Ohtani, Y. Koya, M. Kannagi, N. Yamamoto, and M. Fujii. 1999. Human T-cell leukemia virus type I Tax protein abrogates interleukin-2 dependence in a mouse T-cell line. *J. Virol.* **73**:1271-1277.
18. Jacks, T., L. Remington, B. O. Williams, E. M. Schmitt, S. Halachmi, R. T. Bronson, and R. A. Weinberg. 1994. Tumor spectrum analysis in p53-mutant mice. *Curr. Biol.* **4**:1-7.
19. Jerome, K. R., R. Fox, Z. Chen, A. E. Sears, H.-Y. Lee, and L. Corey. 1999. Herpes simplex virus inhibits apoptosis through the action of two genes, Us5 and Us3. *J. Virol.* **73**:8950-8957.
20. Jones, J. M., L. Attardi, L. A. Godley, R. Laucirica, D. Medina, T. Jacks, H. E. Varmus, and L. A. Donehower. 1997. Absence of p53 in a mouse mammary tumor model promotes tumor cell proliferation without affecting apoptosis. *Cell Growth Differ.* **8**:829-838.
21. Kao, S.-Y., and S. J. Mariott. 1999. Disruption of nucleotide excision repair



- by the human T-cell leukemia virus type 1 Tax protein. *J. Virol.* **73**:4299–4304.
22. **Kishi, S., S. Saijo, M. Arai, S. Karasawa, S. Ueda, M. Kannagi, Y. Iwakura, M. Fujii, and S. Yonehara.** 1997. Resistance to Fas-mediated apoptosis of peripheral T cells in human T lymphocyte virus type 1 (HTLV-1) transgenic mice with autoimmune arthropathy. *J. Exp. Med.* **186**:57–64.
  23. **Lemasson, L., V. Robert-Hebmann, S. Hamaia, M. Duc Dodon, L. Gazzolo, and C. Devaux.** 1997. Transrepression of lck gene expression by human T-cell leukemia virus type I-encoded p40 (tax). *J. Virol.* **71**:1975–1983.
  24. **Levine, A. J.** 1997. p53, the cellular gatekeeper for growth and division. *Cell* **88**:323–331.
  25. **Li, Q., N. Yoshioka, M. Yutsudo, S. Inafuku, K. Aozasa, Y. Kitamura, S. Aizawa, Y. Nishimune, A. Hakura, and G. Kondoh.** 1998. Human papillomavirus-induced carcinogenesis with p53 deficiency in mouse: novel lymphomagenesis in HPV E6E7 transgenic mice mimicking p53 defect. *Virology* **252**:28–33.
  26. **Low, K. G., H. M. Chu, P. S. Schwartz, G. M. Daniels, M. H. Melner, and M. J. Comb.** 1994. Novel interactions between human T-cell leukemia virus Tax and activating transcription factor 3 at a cyclic AMP-responsive element. *Mol. Cell. Biol.* **14**:4958–4974.
  27. **Low, K. G., L. F. Dornier, D. B. Fernando, J. Grossman, K. T. Jeang, and M. J. Comb.** 1997. Human T-cell leukemia virus type I Tax releases cell cycle arrest induced by p16 (INK4a). *J. Virol.* **71**:1956–1962.
  28. **Mayake, H., T. Suzuki, H. Hirai, and M. Yoshida.** 1999. Trans-activator Tax of human T-cell leukemia virus type 1 enhances mutation frequency of the cellular genome. *Virology* **253**:155–161.
  29. **Neuveut, C., K. G. Low, F. Maldarelli, I. Schmitt, F. Majone, R. Grassmann, and K. T. Jeang.** 1998. Human T-cell leukemia virus type I Tax and cell cycle progression: role of cyclin D-cdk and p110Rb. *Mol. Cell. Biol.* **18**:3620–3632.
  30. **Nigro, J. M., S. J. Baker, A. C. Preisinger, J. M. Jessup, R. Hostetter, K. Cleary, S. H. Bigner, N. Davidson, S. Baylin, P. Devilee, et al.** 1989. Mutations in the p53 gene occur in diverse human tumor types. *Nature* **342**:705–708.
  31. **Pise-Masison, C. A., K.-S. Choi, M. Radonovich, J. Dittmer, S.-J. Kim, and J. N. Brady.** 1998. Inhibition of p53 transactivation function by the human T-cell lymphotropic virus type I Tax protein. *J. Virol.* **72**:1165–1170.
  32. **Pise-Masison, C. A., M. Radonovich, K. Sakaguchi, E. Appella, and J. N. Brady.** 1998. Phosphorylation of p53: a novel pathway for p53 inactivation in human T-cell lymphotropic virus type 1-transformed cells. *J. Virol.* **72**:6348–6355.
  33. **Ratner, L., R. C. Griffith, L. Marselle, M. Hoh, F. Wong-Staal, and C. Saxinger.** 1987. A lymphoproliferative disorder caused by human T-lymphotropic virus type I: demonstration of a continuum between acute and chronic adult T-cell leukemia-lymphoma. *Am. J. Med.* **83**:953–958.
  34. **Reid, R. L., P. F. Lindholm, A. Mireskandari, J. Dittmer, and J. N. Brady.** 1993. Stabilization of wild-type p53 in human T-lymphocytes transformed by HTLV-I. *Oncogene* **8**:3029–3036.
  35. **Ressler, S., G. F. Morris, and S. J. Marriott.** 1997. Human T-cell leukemia virus type I Tax transactivates the human proliferating cell nuclear antigen promoter. *J. Virol.* **71**:1181–1190.
  36. **Sakamuro, D., P. Sabbatini, E. White, and G. C. Prendergast.** 1997. The polyproline region of p53 is required to activate apoptosis but not growth arrest. *Oncogene* **15**:887–898.
  37. **Santiago, F., E. Clark, S. Chong, C. Molina, F. Mozafari, R. Mahieux, M. Fujii, N. Azimi, and F. Kashanchi.** 1999. Transcriptional up-regulation of the cyclin D2 gene and acquisition of new cyclin-dependent kinase partners in human T-cell leukemia virus type I-infected cells. *J. Virol.* **73**:9917–9927.
  38. **Sarnow, P., Y. S. Ho, J. Williams, and A. J. Levine.** 1982. Adenovirus E1B-58kd tumor antigen and SV40 large tumor antigen are physically associated with the same 54 kd cellular protein in transformed cells. *Cell* **28**:387–394.
  39. **Schmitt, I., O. Rosin, P. Rohwer, M. Gossen, and R. Grassman.** 1998. Stimulation of cyclin-dependent kinase activity and G<sub>1</sub>- to S-phase transition in human lymphocytes by the human T-cell leukemia/lymphotropic virus type I Tax protein. *J. Virol.* **72**:633–640.
  40. **Spender, L. C., E. J. Cannell, M. Hollyoake, B. Wensing, J. M. Gawn, M. Brimmell, G. Packham, and P. J. Farrell.** 1999. Control of cell cycle entry and apoptosis in B lymphocytes infected by Epstein-Barr Virus. *J. Virol.* **73**:4678–4688.
  41. **Suzuki, T., S. Kitao, H. Matsushime, and M. Yoshida.** 1996. HTLV-I Tax protein interacts with cyclin-dependent kinase inhibitor p16 (INK4a) and counteracts its inhibitory activity towards CDK4. *EMBO J.* **15**:1607–1614.
  42. **Suzuki, T., T. Narita, M. Uchida-Toita, and M. Yoshida.** 1999. Down-regulation of the INK4 family of cyclin-dependent kinase inhibitors by tax protein of HTLV-I through two distinct mechanisms. *Virology* **259**:384–391.
  43. **Thome, K. C., A. Radfar, and N. Rosenberg.** 1997. Mutation of Tp53 contributes to the malignant phenotype of Abelson virus-transformed lymphoid cells. *J. Virol.* **71**:8149–8156.
  44. **Tsukahara, T., M. Kannagi, T. Ohashi, H. Kato, M. Arai, G. Nunez, Y. Iwanaga, N. Yamamoto, K. Ohtani, M. Nakamura, and M. Fujii.** 1999. Induction of Bcl-xl expression by human T-cell leukemia virus type I through NF- $\kappa$ B in apoptosis-resistant T-cell transfectants with Tax. *J. Virol.* **73**:7981–7987.
  45. **Unnikrishnan, L., A. Radfar, J. Jenab-Wolcott, and N. Rosenberg.** 1999. p53 mediates apoptotic crisis in primary Abelson virus-transformed pre-B cells. *Mol. Cell. Biol.* **19**:4825–4831.
  46. **Venkatachalam, S., Y.-P. Shi, S. N. Jones, H. Vogel, A. Bradley, D. Pinkel, and L. A. Donehower.** 1998. Retention of wild-type p53 in tumors from p53 heterozygous mice: reduction of p53 dosage can promote cancer formation. *EMBO J.* **17**:4657–4667.
  47. **Werness, B. A., A. J. Levine, and P. M. Howley.** 1990. Association of human papillomavirus types 16 and 18 E6 proteins with p53. *Science* **248**:76–79.
  48. **Wong, K. S., Y.-J. Li, J. Howard, and Y. Ben-David.** 1999. Loss of p53 in F-MuLV induced-erythroleukemias accelerates the acquisition of mutational events that confers immortality and growth factor independence. *Oncogene* **18**:5525–5534.